# The Use of Variograms in Remote Sensing: I. Scene Models and Simulated Images

CURTIS E. WOODCOCK

*Department of Geography and Center for Remote Sensing, Boston University, 675 Commonwealth Avenue, Boston, Massachusetts 02215*

ALAN H. STRAHLER

*Department of Geology and Geography, Hunter College, City University of New York, 695 Park Avenue, New York, New York 10021*

DAVID L. B. JUPP

*Division of Water Resources Research, C.S.I.R.O, P.O. Box 1666, Canberra, ACT, Australia*

Extraction of information from remotely sensed images would greatly benefit from increased use of spatial data. However, the utility of spatial data has been undermined by a lack of understanding of the nature and causes of observed spatial variation in images. One approach to this problem is to model the spatial variation in images as a function of ground scene and sensor parameters. Variograms are the tool used to link models of ground scenes to spatial variation in images. Explicit variograms are calculated for simple models of ground scenes consisting of randomly located discs on a continuous background. By incorporating the effect of the IFOV of the sensor through a process called regularization, explicit variograms for images of these scene models are derived. Verification of the explicit variograms is accomplished by simulating images that match the assumed scene model and sensor parameters and calculating empirical variograms for these images. For a simple scene model of randomly located discs on a continuous background, explicit and empirical variograms match, verifying the convergence of these two dissimilar approaches. The sensitivity of variograms is studied through varying parameters of scene models both in calculating explicit variograms and in simulating images. Results indicate direct ties between several scene parameters and the behavior of variograms. The height of the sill of the variogram is related to the density of objects. The range of influence is related to the size of objects. Increased variance in the size distribution of objects results in a more rounded shape in the variogram near the sill. Primary effects of increasing the units of regularization, or larger pixel size, are a decrease in the height of the sill and an increase in the range of influence.

## 1. Introduction

As the collection of remotely sensed data has shifted from analog to digital formats, there has been as associated shift from visual to computer-based analysis methods. During this period of roughly the last 15 years, several interesting trends have emerged. First, a tremendous amount has been learned about the spectral properties of surface materials. As a result, techniques that use spectral properties to study surface phenomenon have become highly sophisticated and effective. Not only has there been a great accumulation of data on the spectral properties of a wide variety of objects, but there have been significant advances in the understanding of the causes of these spectral properties. If this first trend can be summarized by asserting that there has been an increase in the use of data from the spectral domain in remote sensing, then a second trend during the same time period can be summarized as a decrease in the use of data from the spatial domain. Visual interpretation of imagery has always relied heavily on texture,


52 Vanderbilt Ave., New York, NY 10017 0034-4257/88/$3.50

or spatial variation in images, for the discrimination of surface phenomenon. However, it has proven difficult to quantify the spatial patterns humans recognize and incorporate them in computer-based methods of information extraction. This is not to imply that there have not been efforts made to include spatial data in image analysis procedures, but compared to the effort devoted to the use of spectral data, the spatial domain has been largely ignored.

One reason spatial data are not used more in remote sensing is that the nature and causes of spatial variation in images are not understood. Certainly most people recognize their existence and potential value in remote sensing, but the lack of understanding concerning their causes has undermined their exploitation. In particular, no one has been able to predict the spatial patterns to be expected for a particular location in a particular type of imagery. Instead, the use of spatial data has been limited to the empirical association between surface phenomenon and spatial patterns in images. The approach taken in this paper is to attempt to understand the nature and causes of spatial variation in images as they relate to the characteristics of ground scenes and the sensor collecting the imagery. An improved understanding in this area is expected to serve as a basis for development of future information-extraction methods that more logically use spatial data.

One distinction that is used throughout this paper concerns the difference between a scene and an image. A *scene* refers to the ground scene from which remotely sensed measurements are derived to create an *image*. In order to study the effects of scenes on the spatial characteristics of images, a systematic method of describing scenes is required. The approach used in this paper follows the description presented by Strahler et al. (1986) that models ground scenes as assemblages of discrete objects arranged on a continuous background.

## 2. Variograms

In this study variograms are used to measure the spatial variation in images. Variograms measure spatial variation in a *regionalized variable*. Any random variable whose position in space or time is known is a regionalized variable. In this formulation, variables are indexed by their location. Thus, assume $Y(x)$ is a regionalized variable associated with location $x$. For the variable $Y$ at different locations, it becomes necessary to index the locations as $x_i$, where $i = 1, \ldots, n$ correspond to $n$ observations. If the $Y(x_i)$ are uncorrelated, then the image will consist of random noise. If however, the $Y(x_i)$ are in some way related, then the data will exhibit spatial structure. Perhaps the weakest assumption one can make about this structure is what Matheron (1971) refers to as the "intrinsic" hypothesis, that the increments $Y(x_i + h) - Y(x_i)$ associated with a small distance $h$ are weakly stationary. Under this assumption, the first moment of the increment, its expected value, is constant or at least only slowly varying with spatial position $x$; and the second moment is also invariant with spatial position. The second moment is called the *variogram*:

$$2\gamma(h) = E\left[Y(x_i + h) - Y(x_i)\right]^2.$$

Just as the variance characterizes the distribution of a nonspatial random vari-

able, so the variogram characterizes the distribution of a regionalized variable. The distance at which samples become independent is often called the range of influence and is denoted as $a$. The value at which the variogram levels off is denoted $c$ and is called the sill (Clark, 1979).

Geostatisticians have used the variogram as a primary tool in many spatial studies. In particular, variograms are used as part of a process called kriging. Kriging is a method of estimating local values from surrounding point samples, a process generically referred to as interpolation. Kriging uses the relationship between point samples established by the variogram to estimate the volume of lodes and efficiently locate additional samples (Matern, 1960). For kriging, a model describing the shape of the variogram is necessary.

One commonly used model for the shape of a variogram is the *spherical model*:

$$\gamma(h) = c\left[3h/2a - h^3/2a^3\right] \text{ when } h \leqslant a$$

and

$$\gamma(h) = c \text{ when } h > a.$$

Figure 1 shows an example of a spherical model of a variogram. As expected, the variogram passes through the origin. If samples are taken exactly zero distance apart, then they are the same sample and their variance will also be zero. As $h$ increases within the range of influence, the difference between measurements increases and the variogram rises. Past the distance $a$, samples from the data are independent, and the variogram reaches a stable plateau at the value $c$, the sill.

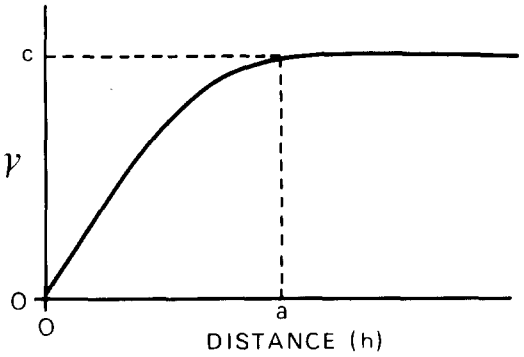


FIGURE 1. The spherical model of a variogram (modified from Clark, 1979)

Just as a sample variance is an estimate of the true variance of a variable, the sill is an estimate of the true variance of a regionalized variable. Thus, one can estimate the sill via a sample variance.

The spherical model is often referred to as the "ideal" model for a variogram because there is a well-defined sill and the meaning of the range of influence is easily interpreted (Clark, 1979). Not all models for the shape of a variogram share these characteristics. Figure 2 shows the shape of an exponential model for a variogram compared with a spherical model with the same sill and range of influence. The exponential model is

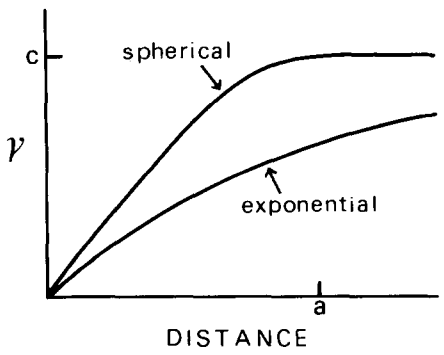


FIGURE 2. The spherical and exponential models for the same values of $a$ and $c$ (modified from Clark, 1979).

calculated as follows:

$$\gamma(h) + c[1 - \exp(-h/a)].$$

The exponential model never reaches its sill, but asymptotically approaches it. In addition, the meaning of $a$, the range of influence, is not clear. In the spherical model there was a direct physical interpretation of $a$, but in the exponential model it is a parameter necessary to describe the shape of the model that has limited interpretive value.

There are models for the shape of variograms which do not have a sill. The simplest form of these is the *linear model*:

$$\gamma(h) = ph,$$

where $p$ is the slope of the line. An extension of this model is the *generalized linear model*:

$$\gamma(h) = ph^{\lambda},$$

where $0 \leqslant \lambda < 2$. Figure 3 shows the effect of the exponent $\lambda$ on the shape of the generalized linear model.

While the above models are commonly used in geostatistics, other models could be used. For example, all the above models are monotonic, assuming that variation will only increase as a function of distance. However, if the data exhibit periodicity, models based on trigonometric functions might be appropriate. Also, variograms can be multidimensional. All the examples have shown one-dimensional (i.e., isotropic) variograms, but two- and three-dimensional variograms are possible. In this situation $h$ becomes a vector specifying both distance and direction (and possibly inclination). One-dimensional variograms have the advantage of being easy to display and interpet. Two-dimensional variograms are usually displayed as contour plots and can be useful for revealing anisotropy in data. However, displays using contours can make evaluation of shapes of variograms difficult. As a third dimension is added there is again potential for information on variation in another dimension, but the problems of display and analysis of shape increase.

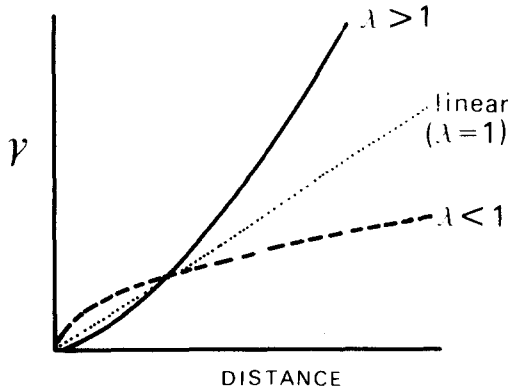


FIGURE 3. The linear model and generalized linear models of variograms (modified from Clark, 1979).

In geostatistics, the models used to describe variograms tend to be combinations of several models. These combinations can include several models of the same type with different parameters, or different types of models. The use of combinations of models is similar to Fourier analysis where sinusoidal curves with different amplitudes, frequencies, and phases are combined to model a function (Bloomfield, 1976). One difference from Fourier analysis is the subjective nature of methods used to determine the type of models to be combined and their coefficients. Often the nature of the model selected is guided by the specific interests of an application. Criteria which affect model selection are the behavior near the origin, the fit near the sill, and the de-

termination of the range of influence (Clark, 1979).

### 2.1. Scene models and variograms

The previously described models for the shapes of variograms are necessary for kriging, and as a result have played a significant role in studies involving variograms. However, for the purpose of understanding spatial variation in remotely sensed images, their value is limited. The reason is that there is no apparent way to link models for the shapes of variograms to scene models. A more useful tool is a variogram whose characteristics can be determined as a function of the parameters describing a scene model. Serra (1982) provides a method for calculating explicit variograms for some simple scenes.

The derivation of explicit variograms is based on an extension of the binomial. This approach is well suited for a discrete scene model, in which the objects in the scene and the background are considered homogeneous, thus allowing only two states in the image. It is possible to determine $q$, the proportion of the area not covered by $N$ randomly distributed objects of area $b$ within a large area $A$ as

$$q = \exp(-Nb/A).$$

The proportion of the area covered by objects is simply $1 - q$. The variogram for the distance between two points $h$ distance apart is

$$\gamma(h) = q - \exp\left[\frac{N}{A}(O(h) - 2b)\right]$$

where $O(h)$ is the overlap function. The overlap function for the case of randomly located, overlapping discs of radius $r$, when $h < 2r$ is

$$O(h) = 2r^2\cos^{-1}\left[\frac{h}{2r}\right] - \sqrt{r^2 - h^2/4}.$$

If $h \geq 2r$, then no overlap occurs and $\gamma(h) = q(1-q) = qp$, which is the binomial variance.

This formulation of a variogram is slightly different than originally described. In the original description, the variable $Y(x)$ is continuously measured. For this explicit variogram, the variogram is defined as the probability the $Y(x)$ and $Y(x+h)$ will be different, i.e., $x$ is located within the object and $x+h$ is located on the background, or vice-versa. This is equivalent to the probability of crossing a boundary between an object and the background.

Figure 4 shows explicit variograms for scenes of overlapping discs. The variogram is calculated for $N = 1$, 10, 25, 50, 100, and 200 objects of unit radius on an

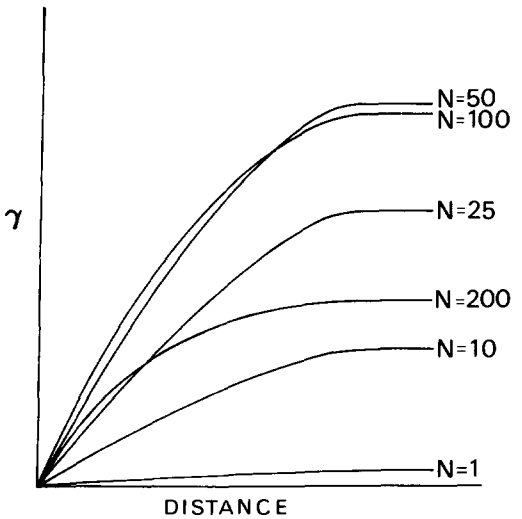


FIGURE 4. Variograms for scenes with different numbers ($N$) of randomly located, overlapping discs.

area of size 100 $\pi^2$ units. The variogram starts with zero variance and rises to the sill, or maximum variance. The distance to the sill is the size of the objects, and the height of the sill is determined by the number of objects. At low values of $N$, variance is low because most of the area is background. As $N$ increases, the curves become steeper and the sill successively higher until half the area is covered ($p = q = 0.5, N = 69.3$). As more than half of the area is covered, the height of the sill decreases because more of the area becomes covered by discs. Thus, there will be two different scenes with the same sill, one in which the discs occupy area $p$ and one in which the background occupies area $p$. Distinguishing between these two alternatives should not normally present a problem because the general brightness of the scene will be different.

The two cases may also be distinguished by their shape. Note that in Figure 4 the variograms for $N > 69.3$ have a more rounded shape than those for $N < 69.3$. The reason for this may be resolved by studying another of the useful measures of variograms, the slope at the origin. Serra (1982) shows that the slope at the origin depends on the amount of boundary between discs and the background. This reduces for both high and low $N$, but in different ways. For higher values of $N$, the background becomes dissected into a large number of small areas, or slivers between the discs. In this situation the amount of boundary becomes large, and $\gamma(h)$ becomes large at short distances, leading to the more rounded, faster rising shape of the variogram for large $N$. A more complete treatment of the mathematical theory underlying variograms has been presented in an earlier paper (Jupp et al., 1988).

### 2.2. Variograms and remotely sensed images

Whenever remotely sensed data consist of images, an important new information component is added to the measurement output by the sensor: its spatial position. Since the position of the measurement in the image is usually a quantifiable function of the position in the scene of the resolution cell from which it is derived, each measurement can be associated with a ground location and be positioned relative to other measurements. The sensor's response then becomes a regionalized variable, because its position in space is known. Thus, variograms can be used to characterize the spatial structure in remotely-sensed images.

There is an important factor that must be considered when using variograms in conjuction with remotely sensed images. The models presented for the shapes of variograms (spherical, exponential, etc.) are for *punctual* variograms, or variograms derived from point measurements. Measurements in remotely sensed images are integrated over areas, and this difference is important. In this instance, when measurements are taken over some length or area, the resulting variogram is referred to as *regularized*. Regionalized variables can be thought of as having a true or underlying punctual variogram based on point measurements, and an associated regularized variogram which is derived from measurements taken over a given length or area.

In remotely sensed images, the regularizing area is the instantaneous field of view of the sensor, with the point spread function describing the form of the regularization. For this study, the resolution-cell size of the image is taken as the units

of regularization. The effects of regularization are similar to those typically associated with measurements that represent some form of aggregation. The overall variance of the data is reduced, and fine scale variations are blurred. Certainly variation at a scale finer than the scale of regularization cannot be detected and variations less than two to three times the scale of regularization cannot be reliably characterized.

The effect of regularization on punctual variograms can be determined analytically, but is considerably more straightforward for some models. Geostatisticians have determined the expected results of one-dimensional regularization for several models of variograms for use with core samples (Clark, 1977). The exponential model for samples of length $l$ is

$$\gamma_l(h) = C\left\{\frac{2a}{l} + \frac{a^2}{l^2}\left[1 - e^{-l/a}\right] \times e^{-h/a}\left[1 - e^{l/a}\right]\right\},$$

where $h \geq l$. Determination of $\gamma_l$ when $h < l$ is considerably more complex.

The linear model is straightforward for all distances:

$$\gamma_l(h) = \frac{ph^2}{3l^2}(3l - h) \text{ when } h \leq l$$

and

$$\gamma_l = p(h - l/3) \text{ when } h > l.$$

The calculation of a regularized spherical model is complicated, and tables have been produced to aid in its estimation. The sill for the regularized variogram will be lower than the punctual variogram, as can be seen in Fig. 5.

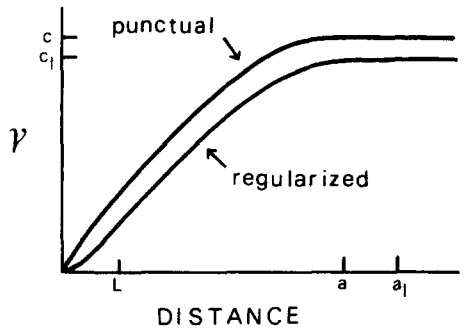


FIGURE 5. The effect of regularization from samples of length $l$ on the spherical model of a variogram (modified from Clark, 1979).

The effect of regularization of disc-model variograms can be seen in Figs. 6A–H and Fig. 7. These figures show the punctual variogram and the regularized variogram for several different units of regularization for the same scene model. The punctual variogram is the same for these figures, but the units of regularization are increased in size. In essence, increasing the units of regularization is analogous to coarser spatial resolution in remotely sensed imagery. The scene model used in these tests is randomly distributed discs of radius 3.5 m that cover 10% of an area of size 360×360 m.

Figures 6B–H show variograms as they would look if calculated from remotely sensed imagery at various spatial resolutions. In other words, the $x$-axis is in integer multiples of the units of regularization. As a result, the scale of the $x$-axis changes in these graphs. At small units of regularization, the variograms resemble the punctual variogram, with a well-developed drop from the sill in the range of influence. At larger units of regularization, the shape of the variogram

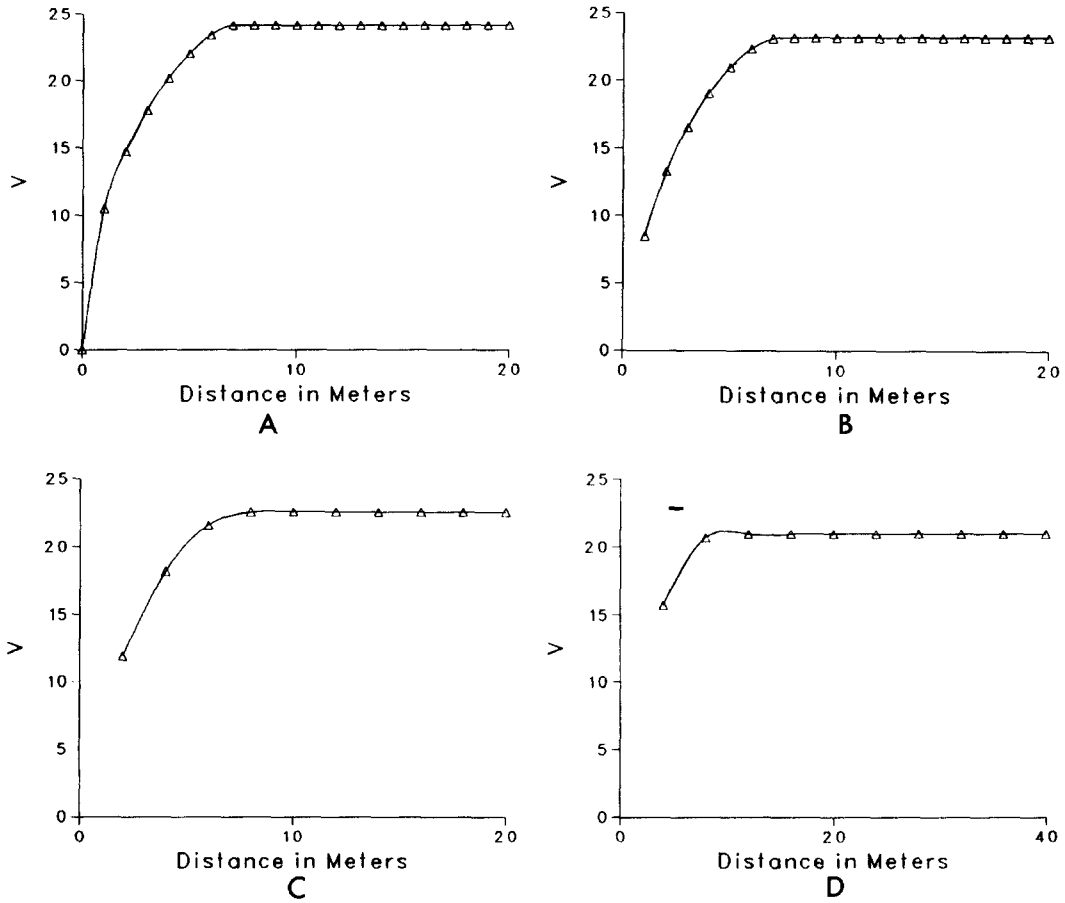


FIGURE 6. The effect of regularization on a disc model variogram. All variograms are for the same scene model but each use a different level of regularization. B–H are displayed as if measured from a remotely-sensed image. A) Punctual variogram; B) 1-m regularization; C) 2-m regularization; D) 4-m regularization; E) 6-m regularization; F) 8-m regularization; G) 12-m regularization; H) 30-m regularization.

becomes very simple. In fact, for Figs. 6D–F, or 4, 6, and 8 m, the variogram is essentially one point below the sill. By 12 m and beyond the variogram is essentially flat. Figure 7 is a composite of the graphs in Figs. 6A–F that holds the $x$-axis constant. This composite illustrates several important points about the effect of regularization. As the size of the regularizing units increase, three things should be noted. First, the height of the sill (or the variance of the variable) decreases. Second, the range of influence, or the distance to the sill, increases. Third, the height of the variogram at the first measured interval of $h$ increases relative to the sill until they match. While one can determine the regularized variogram from the punctual variogram, in practice, the more common situation is that the observed variogram is a regularized variogram and the desired form is the punctual variogram. In this situation, the equation for the regularized variogram is used to estimate $a$ and $c$, which are then used in the equation for the punctual

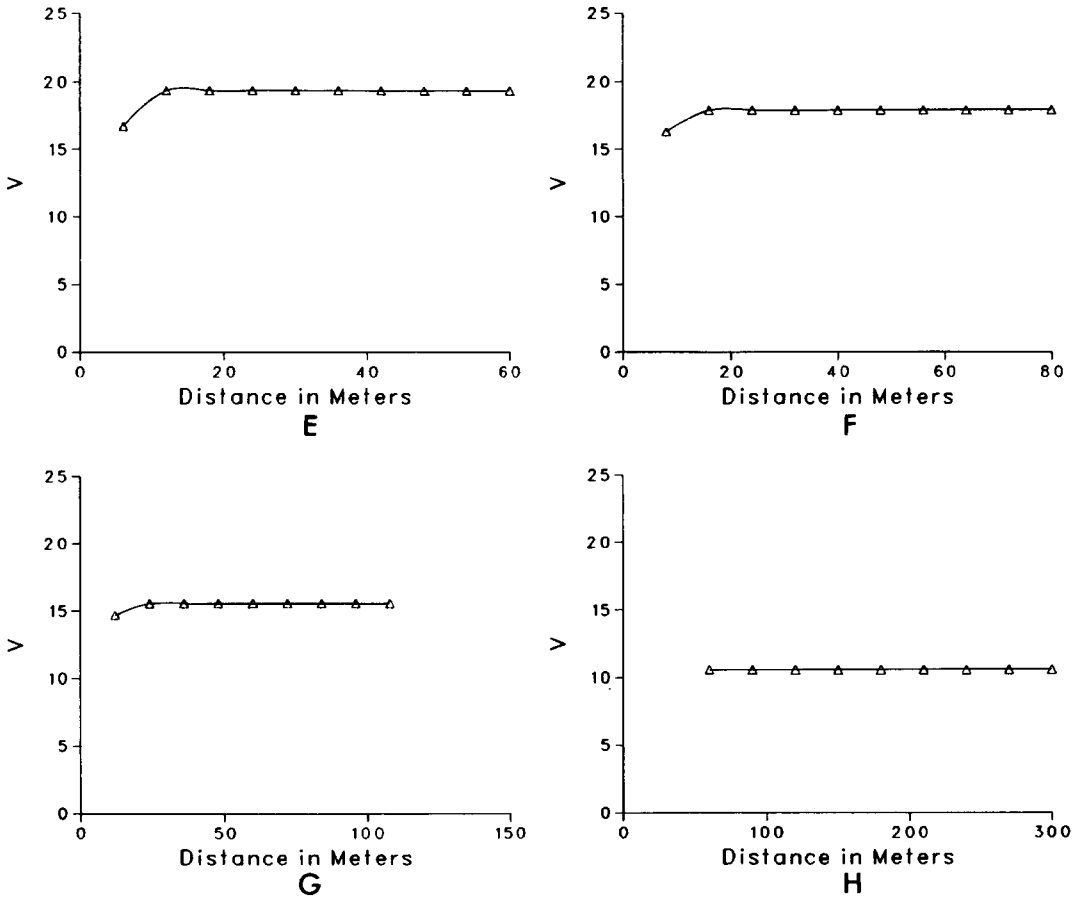


FIGURE 6. (Continued)

variogram. A more thorough mathematical treatment of regularization can be found in Jupp et al. (1988).

Variograms can be calculated from remotely sensed images as follows:

$$2\gamma(h) = \frac{1}{n} \sum_{i=1}^{n} [Y(x_i) - Y(x_i + h)]^2,$$

where $n$ is the number of observations used to estimate $\gamma$. Ideally, a variogram should be computed by comparing each point with all others. In a normal application in geostatistics, the number of available samples is limited, and an estimate of the variogram is produced in this way. In the remote sensing case, generally the area of interest is entirely sampled; but, due to the large sizes of images, the comparison of each measurement with all other measurements is computationally unrealistic, and constraints need to be imposed. One constraint concerns the distance $h$ over which the variogram is to be measured. This distance can be thought of as a "window size" when using image data and needs to be larger than the range of influence and large enough for any periodicities in the data to be revealed.

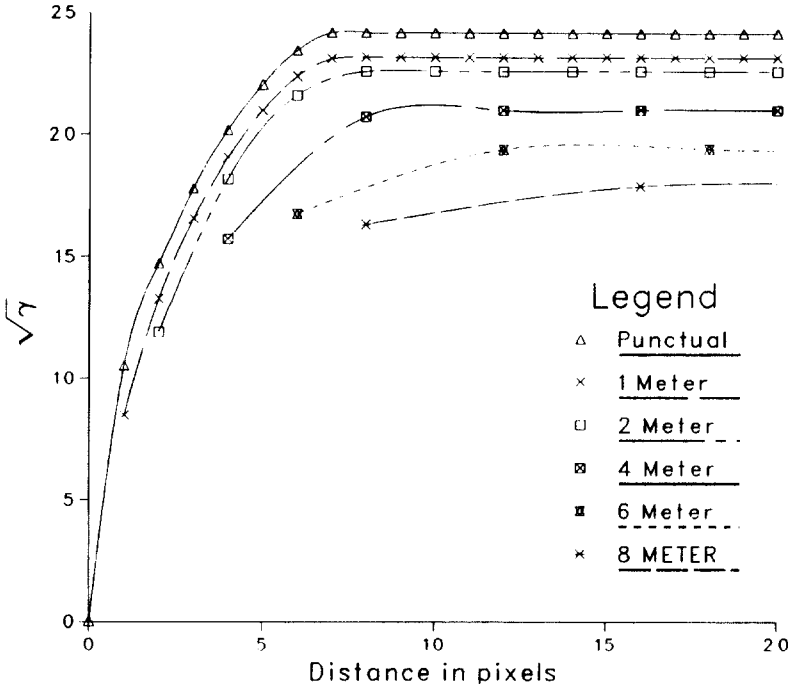


FIGURE 7. The effect of regularization on a disc model variogram. This graph is a composite of Figs. 6A–F that holds the $x$-axis constant.

A second constraint concerns the number of points in the image to be used as centers of windows. The use of a sample results in an estimate of the true regularized variogram. The actual locations of points to be used are determined randomly from the set of points greater than distance $h$ from the edges of the image. This restriction is to avoid boundary conditions and to insure a constant number of points contributing to the two-dimensional variogram for each vector $h$. For the one-dimensional variogram, there are not the same number of pixels for each distance $h$. In fact, the possible combinations of distances between centers of pixels grows as their distance apart increases. To simplify the resulting variogram, all distances between successive integer multiples of the number of resolution cells are combined to produce a single estimate of $\gamma$ over that interval. The distance used to index this estimate is the average of the contributing distances weighted by their frequency of occurrence. For example, there are four pixels 1 resolution-cell distant from any center point (its nearest neighbors), and four pixels 1.414 resolution cells away (at the diagonals). Thus, for the one-dimensional variogram, the contributions of these eight pixels is used at each center point to estimate the value of $\gamma$ for $1 \leqslant h < 2$ units of distance. The distance used to index their result is $\frac{1}{2}(1+\sqrt{2}) = 1.212$, or the average of the distances of the contributing pixels. As $h$ increases, the combinations become more complicated, and the number of pixels contributing to the estimate of any given interval increases. One additional note is that the square root of the variogram is used for all graphs

of observed variograms. In much the same way that a standard deviation is more easily interpreted than a variance, the magnitude of the square root of the variogram is more easily understood.

Variograms were selected for use in this study primarily because of their mathematical simplicity and ease of interpretation. However, other choices exist that would have led to similar results, and deserve some mention. The use of spatial autocorrelation with geographic (Glass and Tobler, 1971; Olson, 1975) and time series (Kisiel, 1969) data is closely related to the use of variograms. Spatial autocorrelation is a measure of covariance between observations divided by the variance of the variable. The correlogram, which measures autocorrelation as a function of distance, is very similar to the variogram (Cliff and Ord, 1981).

Craig and Labovitz (1980) measured autocorrelation in Landsat MSS images and tested the influence of factors related to the sensors, physical factors such as sun angle and cloud cover, and a "geographic location" factor. Their results indicated that the spatial autocorrelation in MSS images cannot be attributed to electromechanical features of the scanner system. Cloud cover and geographic location had significant impacts on the observed autocorrelation in images. In addition, a Box and Jenkins (1976) Autoregressive-Integrated-Moving-Average [ARIMA (1,0,1)] model was found to fit the MSS data. Labovitz et al. (1981) extended the study and found physiography contributed more significantly to autocorrelation in images than land cover. Also, autocorrelation was found to be higher in images with finer spatial resolution (30 m).

There are a couple of minor differences between the correlogram and the variogram. Due to the correction of covariance by the variance, the correlogram intersects the $y$-axis at unity, rather than the origin. Deviations from zero, rather than the sill, are of interest in correlograms. The autocorrelation formulation, and thus correlograms, require a slightly more restrictive stationarity assumption than variograms. The mean is assumed to remain constant over the entire extent of the variable, while the use of variograms only requires that the mean is locally stationary. The use of deviations from the mean in the calculation of covariances requires the more strict assumption of stationarity.

There are reasons to believe that the mean of remotely sensed images will change spatially within a single image. The illumination and reflection geometry is not constant for all resolution cells in an image. Due to the anisotropic reflectance of surface materials, there can be systematic changes in brightness across images. The inappropriateness of the stationarity assumption could lead to biased estimates of the magnitude of autocorrelation. While the general formulation of autocorrelation requires the use of means in the calculation of covariances, in fairness, Geary's coefficient does not and may have been an acceptable alternative for the remote sensing case (Cliff and Ord, 1981).

A second factor that influenced the decision to use variograms rather than autocorrelation approaches concerns the nature of past research on the two methods. Research on autocorrelation has largely been concerned with statistical distribution of autocorrelation coefficients (Cliff and Ord, 1981) and significance testing (Oden, 1984). Other than providing a more objective method of determin-

ing the range of influence, significance testing would not be particularly helpful in this study. The concern for shapes of variograms was considered an attractive feature as the shapes of observed variograms might prove helpful in understanding the relation between spatial variation in images and scene models.

Another choice for a method of measuring spatial variation in images is Fourier analysis. In particular, the power spectrum, which is a plot of the percent variance associated with each frequency as a function of frequency, would have been appropriate (Rayner, 1971; Mollering and Rayner, 1981). This method is mathematically equivalent to the autocorrelation approach, as they are transforms of each other.

Other factors supported the selection of variograms for use in this study. The ability to use Serra's work to explicitly derive variograms for simple scene models is particularly important. There has been work on simulating autocorrelated surfaces (Haining et al., 1983) that might have been useful, but a direct tie to a scene model has not been explicitly developed. A second area of research on variograms that is very useful concerns regularization. Due to the obvious influence of spatial resolution on spatial variation in images, a direct understanding of the effect of the size of the sampling unit on variograms was useful (Jupp et al., 1988). It should also be noted that variograms are similar to many of the texture measures used in remote sensing. These texture measures are often used as features in classification and, like the variogram, measure variance as a function of either distance or direction (Weszka, et al., 1974; Haralick, 1979; Shih and Schowengerdt, 1983; Frank, 1984). One measure, the polarogram (Davis, 1981), is very similar to the two-dimensional variogram, using polar coordinates to plot variance.

## 3. Image simulation

In the last section, two diverse approaches to variograms were presented. One approach is empirical, in which a variogram is calculated from an observed image. The other is theoretical, with the expected nature of variograms being explicitly defined on the basis of a simple scene model. In an effort to bridge the gap between these two approaches, images were simulated on the basis of known scene models. These simulations serve several purposes. First, they confirm the validity of the explicit variograms through empirical testing. Second, they allowed for testing of the extension of the simple disc model to more complicated scenes. And third, the variograms of simulated images help explain the characteristics of empirically calculated variograms from real remotely sensed images.

### 3.1. Simulation methods

The simulated images used in this paper are based on a coniferous forest scene model. The basic approach is a modification of a Monte Carlo computer model used by Li and Strahler (1985) in their studies of forest canopy reflectance. Monte Carlo methods are used to locate trees on a plane which are illuminated from a specified angle and azimuth. This approach leads to four kinds of objects in the scene: illuminated tree crown and background, and shadowed tree crown and background. The forest simulation

represents a general model with several parameters. For this project, these parameters are calibrated primarily by field data collected in the Klamath National Forest in northern California (Li and Strahler, 1985).

In the original model of Li and Strahler, many realizations of individual resolution cells were simulated. Their approach specifies two levels of resolution: 1) the scale at which scene objects are differentiated, and 2) the size of the resolution cells. For this project, the simulation program was altered to simulate one larger scene in which the scale at which scene objects are differentiated matches the size of the resolution cells. The size used in the simulations presented is 1 m. The distinction between a simulated scene and simulated image is minor in this case. A scene implies different objects and an image implies reflectances (or emittances). The simulation assumes no atmospheric effects and a square wave response on the part of the sensor. As a result, there are only four values for reflectances in the image, one for each type of scene element.

The primary parameters of the simulation concern the characteristics of trees: their number, location, size, and shape. In the Li and Strahler model, the number of trees in a single realization of a resolution cell varies according to a Poisson or Neyman Type A distribution. However, for the single realization of a larger area, a single value, or the mean of a Poisson distribution is used to determine the number of trees for the entire area.

Of more interest is the manner in which the trees are located within the scene. Considerable effort has been devoted to this question, and several alternatives have been considered. Li (1981) measured the spatial patterns of trees using point-pattern techniques based on locations derived from aerial photography and found that a Neyman Type A model fit better than the random model. In a later study in a neighboring area, Franklin et al. (1985) again used locations of trees taken from aerial photography and found that the random model was a good approximation. Results of field data collected in the Klamath National Forest indicate that the random model is a reasonable approximation. Thus, in the simulations presented, the locations of the center of trees are determined through random coordinates.

The model is based on the use of cones as the shapes of trees. Thus, the model is limited to coniferous forests. Trees are assumed to have a constant apex angle of 10°, which is based on the field data previously mentioned. A log-normal distribution of the sizes of trees is used. This decision is based on the results of other published studies, and the parameters of the distribution were calibrated from the field data collected in the Klamath. For a more complete description of the model and its parameters, see Li and Strahler (1985).

### 3.2. Validation of the explicit variograms

One use of the simulated images was to validate the explicit variograms. Due to the nature of the forest simulation model it was easily generalized to correspond to the disc model used for the explicit variograms previously presented (Fig. 4). By reducing the variance of the heights of trees to a number close to zero, and eliminating shadows through the use of a solar zenith angle of zero, an image corresponding to discs on a background at 1-m

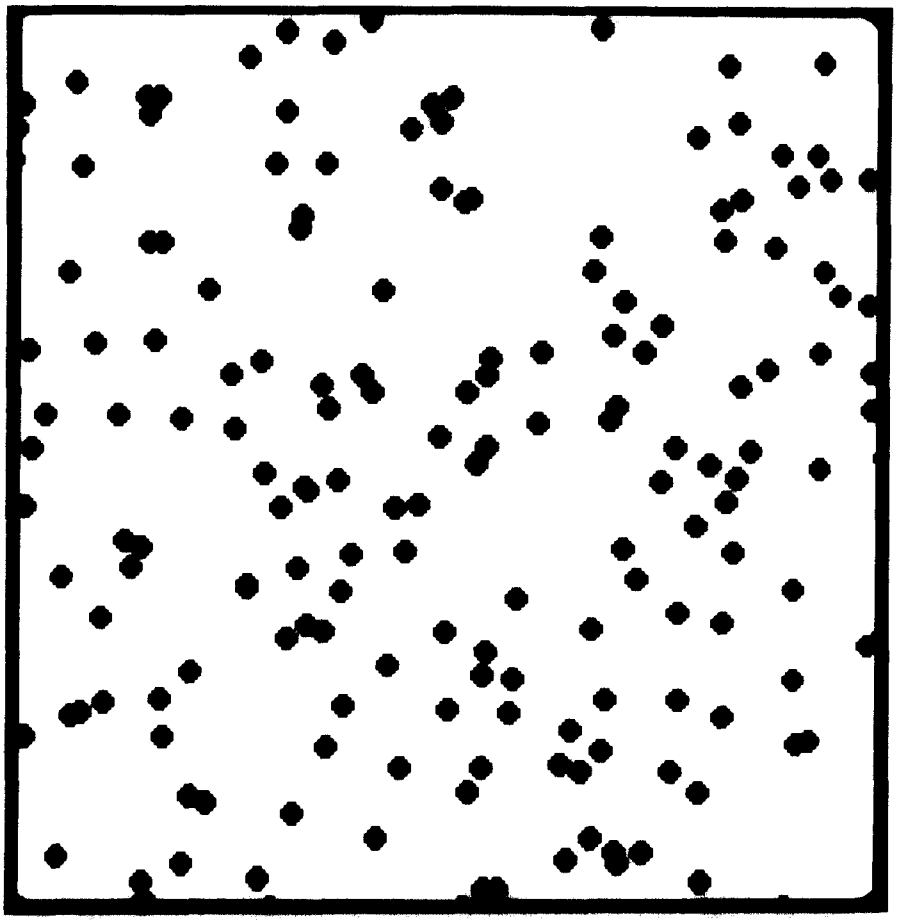

A

FIGURE 8. A portion of the simulated disc image (A) and an enlargement (B).

regularization was simulated. Figure 8 shows the simulated disc image, which has discs of 7-m diameter covering 9.92% of the background of an area 360 × 360 m in size. In order to test the validity of the explicit variograms, an empirical variogram was calculated from the simulated disc image, and an explicit variogram for the corresponding scene model was calculated at 1-m regularization. Figure 9 shows these two variograms plotted together for comparison. These two variograms do not match exactly, but are very close.

There are several possible reasons why the observed and expected variograms do not match exactly. The empirical variogram is derived from one realization of a simulation process based on randomization. Thus, it is likely that this one realization will depart from the model to some extent. Also, the empirical variogram is estimated, in this case from a sample of 600 points in the image. As the number of points is changed, the variogram changes slightly. Clearly, the more points that are used, the more stable and accurate the estimate is likely to be. Fig-

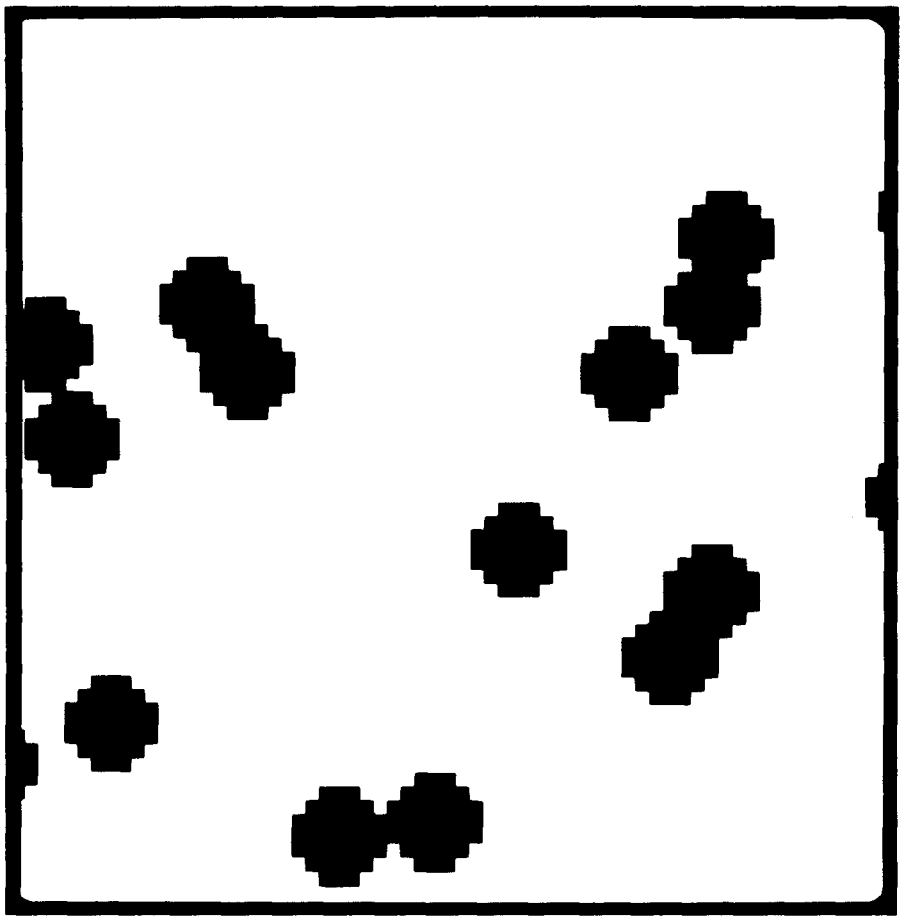

B

FIGURE 8. (Continued)

ure 10 shows four estimates of the variogram for the simulated disc image using four different sampling densities. Their variation is large relative to the difference between the explicit and empirical variograms shown in Fig. 9.

The ability to reproduce empirically through image simulation the results for a disc model expected by theoretical formulation is a significant step in the use of variograms to study spatial structure in images. This "closing of the loop" validated the theory as well as the software used to calculate explicit variograms and estimate variograms from observed images.

### 3.3. Extension of the disc model

Having demonstrated the connection between observed variograms and theoretical variograms using a simple disc model, it is possible to test the effect of variations in that model on variograms. Obviously, real scenes are not composed of randomly located discs of the same size on a uniform background. However, it may be possible to use the characteristics

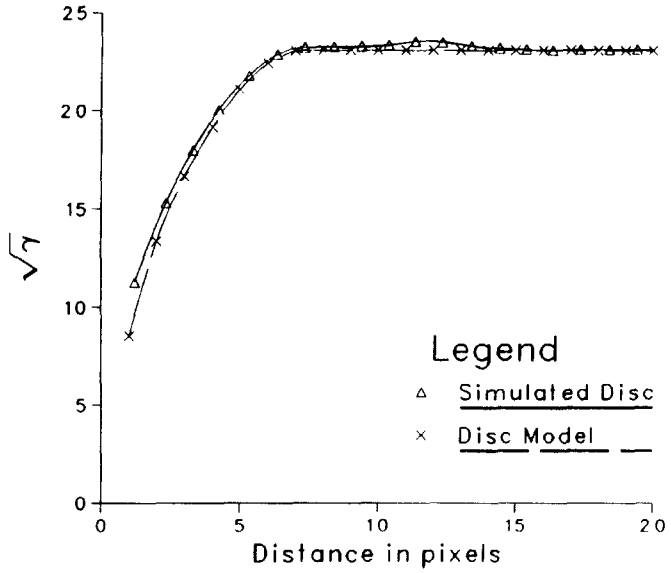


FIGURE 9. Comparison of an explicit variogram and an empirically calculated variogram for the same scene model. The empirical variogram was calculated from the simulated image in Fig. 8.

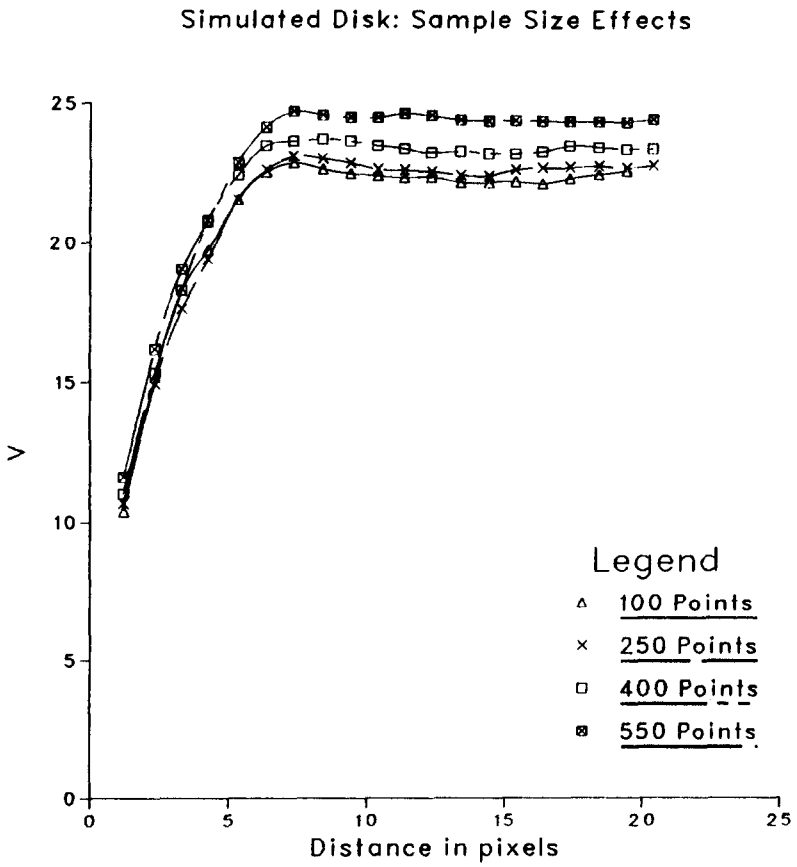


FIGURE 10. The effect of sampling density on empirically estimated variograms.

of explicit variograms from this simple model to help explain the nature of variograms derived from real images.

*3.3.1. Shape.* To test the effect on observed variograms of the shape of objects, a forest image was simulated using the previously described methods. The same parameter settings that were used for the simulated disc image (Fig. 8) were used with one exception; the angle of illumination was changed to 20° in order to produce shadows. The resulting image (Fig. 11) exhibits all four components of the forest model: illuminated canopy, shadowed canopy, illuminated background, and shadowed background. The size of the discs used in calculation of the explicit variogram match the area of the cones in the image. In order to compare the observed variogram from this image with the disc model, it was necessary to convert the image to only two values, or tones. In this instance, trees and shadows were stretched to black and the background was left white. The resulting image (Fig. 12) looks like cones on their

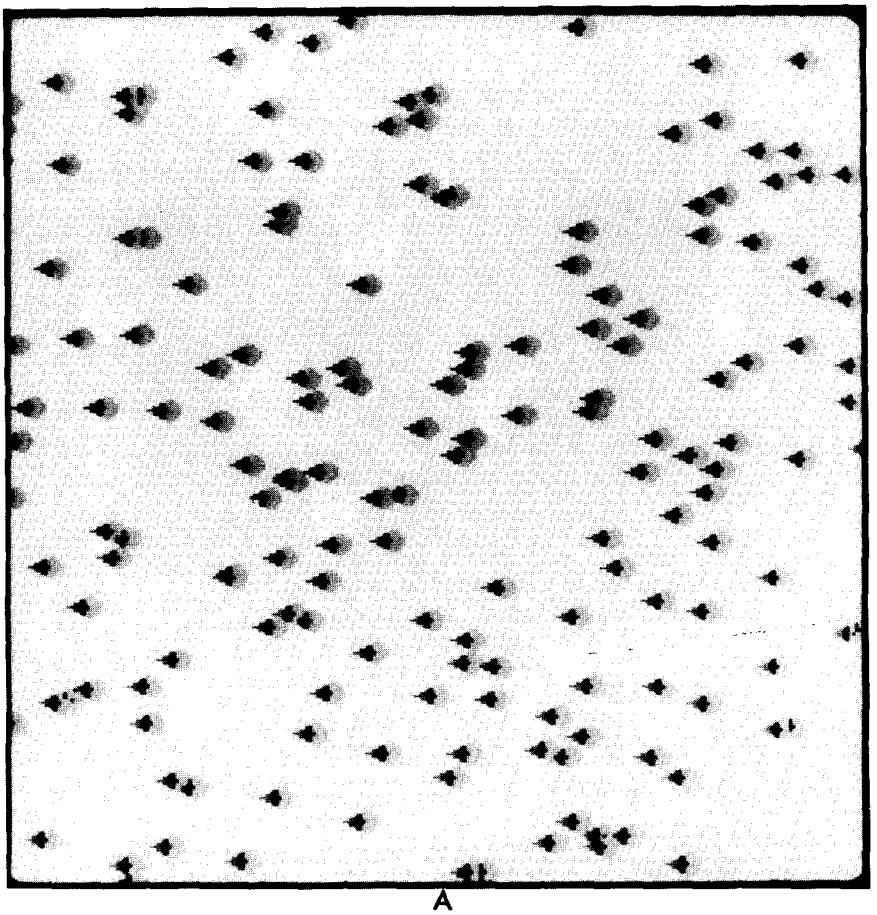


FIGURE 11. A portion of the simulated forest image (A) and an enlargement (B).

sides. These cones do not strictly match the disc model due to their shape, but the ability to extend the disc model is of interest in this case.

A variogram was calculated from the observed black and white image for comparison with the result of the explicit variograms for the disc model. However, it was not clear what values should be used for the disc model in the calculation of the explicit variogram. In particular, it was not obvious what should be used as the size parameter. For the forest cone image, the radius changes as a function of orientation from 3.5 m across the tree to 5.5 m from the far edge of the tree to the tip of the shadow. Figure 13 shows the observed variogram calculated from the image in Fig. 12 compared with three explicit variograms for the disc model using 3.5, 4.5, and 5.5 m for the radii of the discs. Interestingly, the 3.5 m radius is the best approximation of the forest model, which is the same size as the trees before the addition of their shadows. The shadows markedly affect their shape but

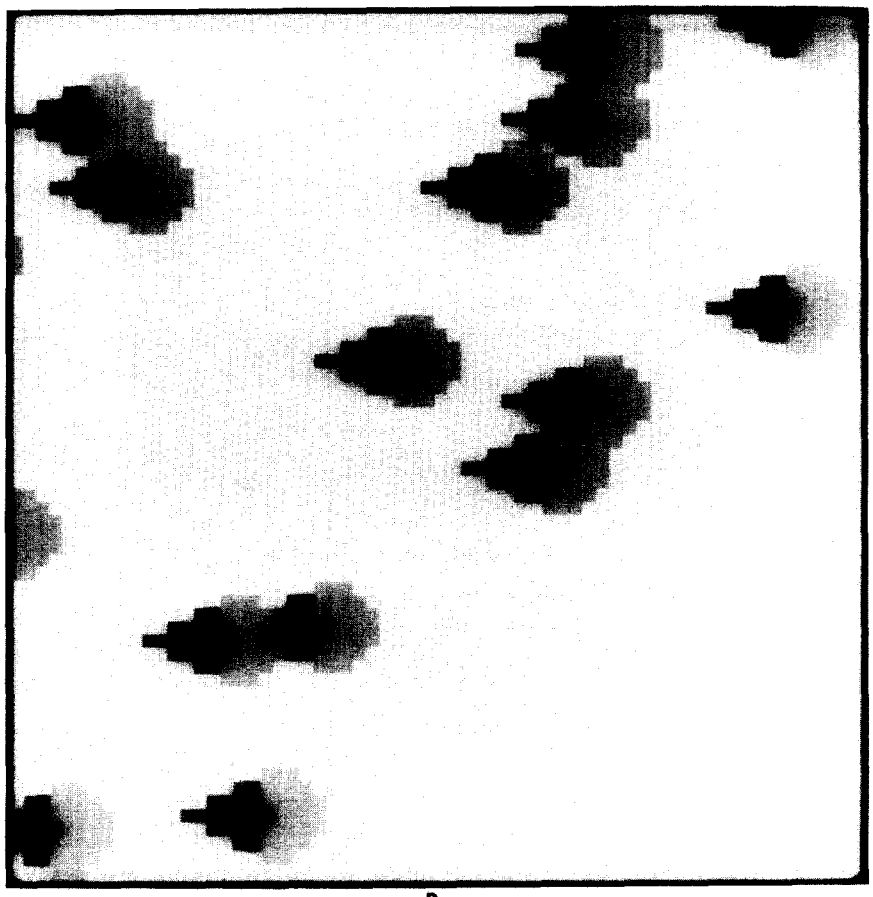


FIGURE 11. (Continued)

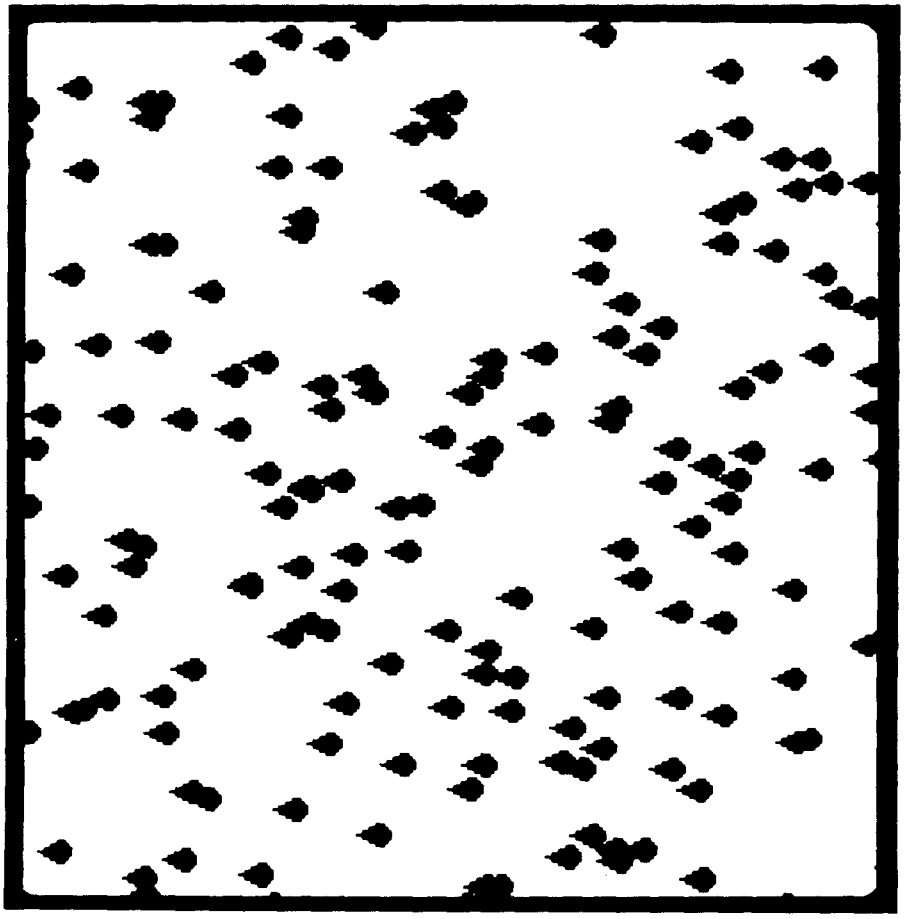

A

FIGURE 12. A portion of the simulated forest image stretched to two tones (A) for comparison with the disc model and an enlargement (B).

do not significantly influence their effective size. Figure 14 is a comparison of the observed variogram with a variogram for discs with area equal to the area of the forest cone. While these two variograms are not a perfect match, they demonstrate that shape is a relatively minor factor in this case. Using just the area covered by individual objects, it was possible to produce a reasonable fit with the disc model. This result is important because it indicates that the disc model might be used as a reasonable approximation of scenes with objects of other shapes.

3.3.2. *Size variance.* The derivation of the explicit variograms assumes that all the discs are the same size, which is unlikely for real scenes. To test the influence of variance in the size of discs, an image was simulated using the same parameters of the initial simulation of the disc image (Fig. 8) with the exception of the variance in disc size. As mentioned earlier, a log-normal distribution is used

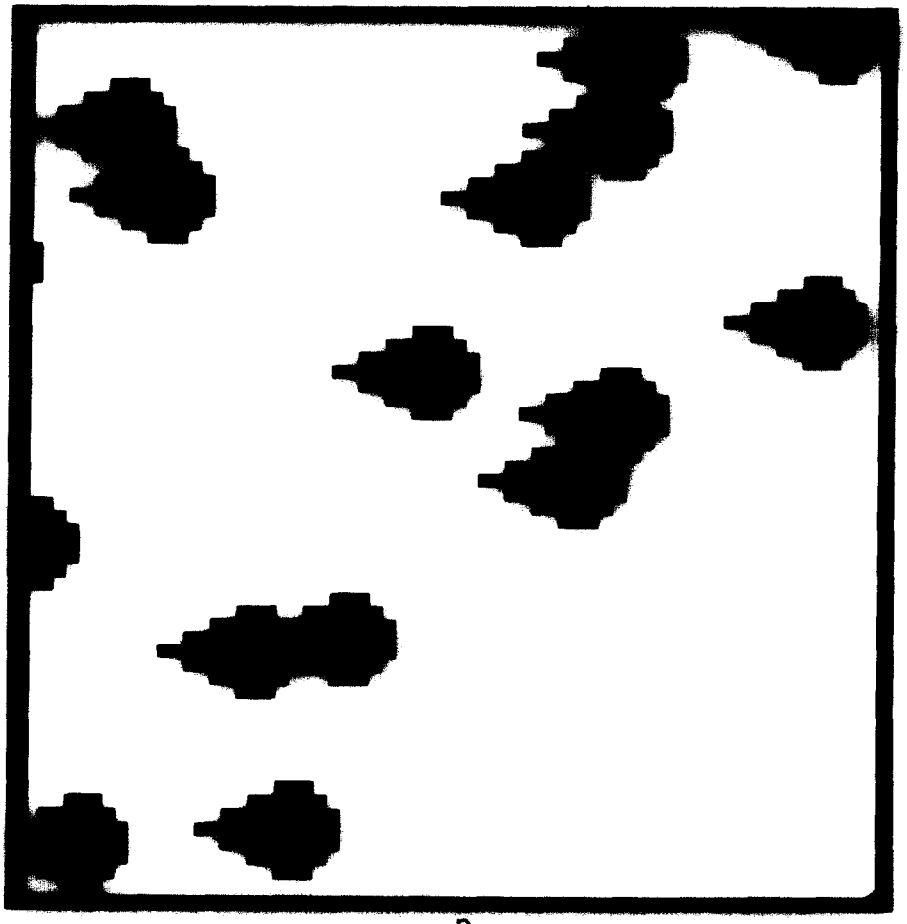

B

FIGURE 12. (Continued)

to describe the size distribution, and its standard deviation was set intentionally high at 3.168. The resulting image is shown in Fig. 15. To calculate an explicit variogram for comparison, it was again necessary to determine the appropriate size to be used for the discs. The mean radius is not a good approximation as the area covered is related to the square of the radius, not the radius. Instead, a value for the radius that produces the same area covered by discs as the log-normally distributed discs would be appropriate. This radius can be calculated using the mean ($m$) and variance ($s^2$) of the log-normal distribution:

$$r = \sqrt{m^2 + s^2}.$$

For the simulated image shown in Fig. 8, the appropriate radius for use in the disc model is 4.72 m.

Figure 16 is a comparison of the observed variogram from the simulated image with a lognormal distribution of disc sizes and the equivalent explicit variogram for fixed size discs. The two

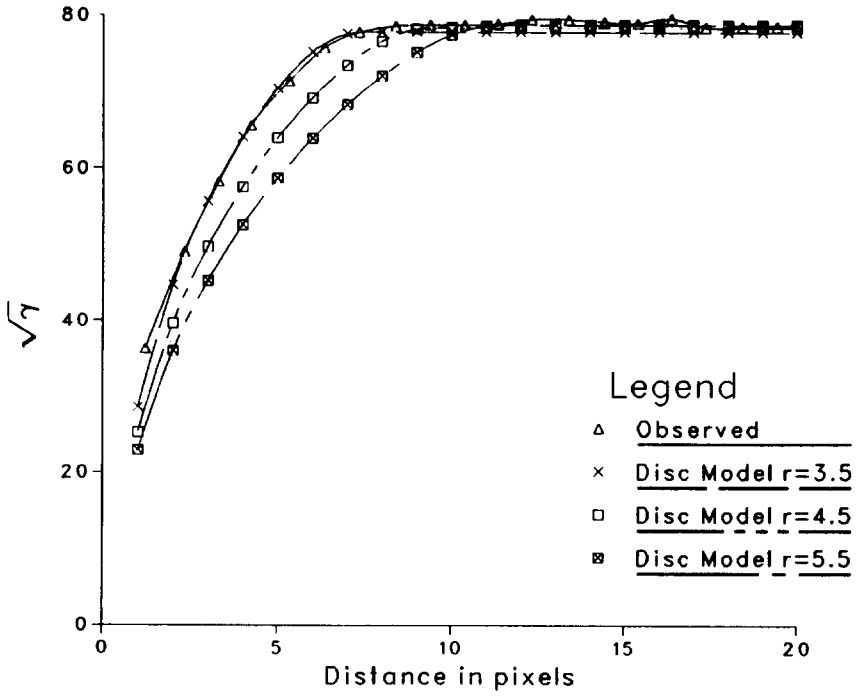


FIGURE 13. Comparison of the observed variogram from the simulated forest image with three disc model variograms for different size discs.

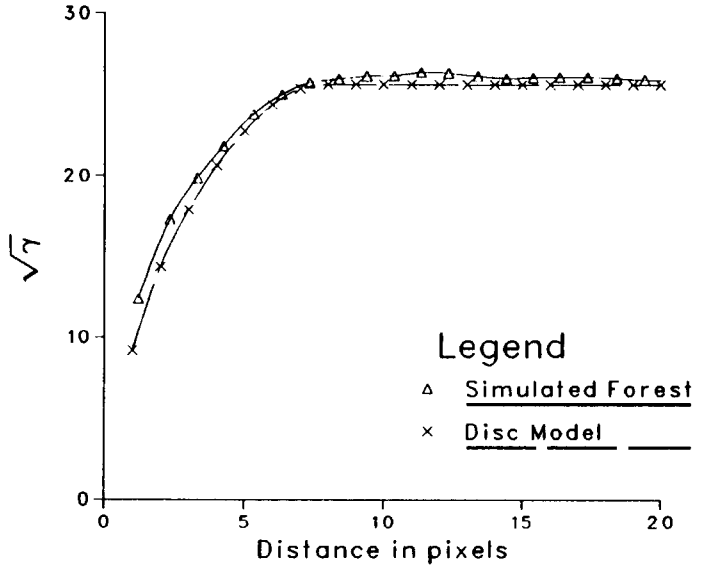


FIGURE 14. Comparison of the observed variogram from the simulated forest image and the disc model.

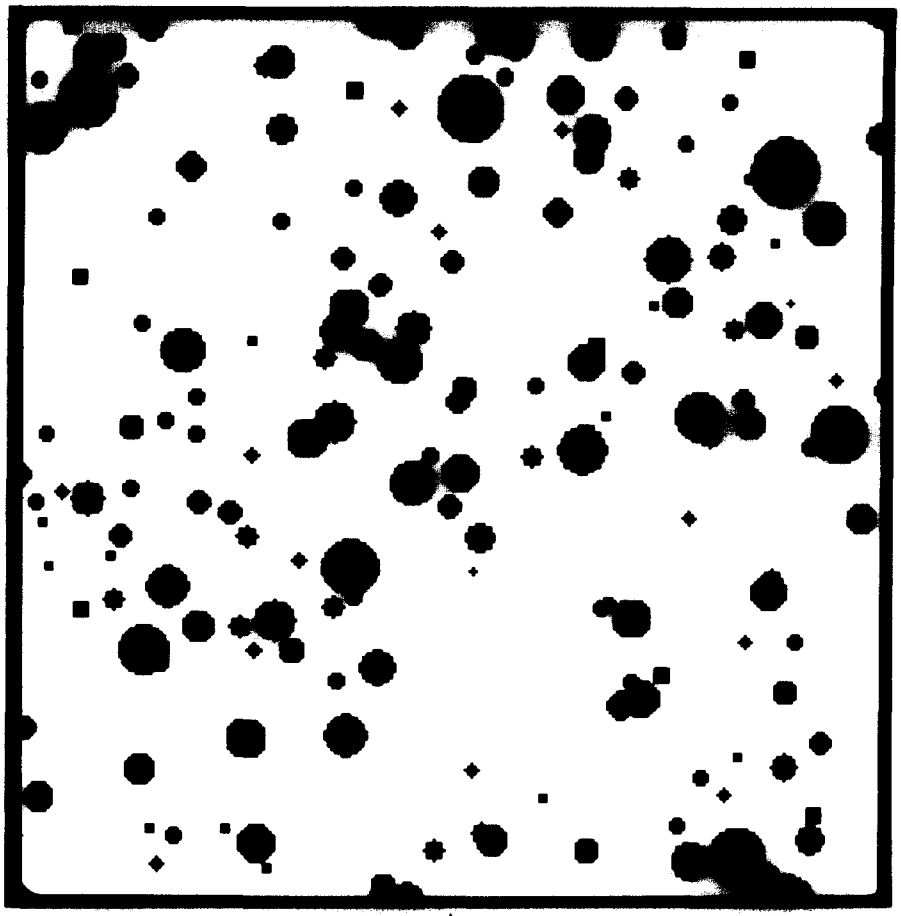


FIGURE 15. A portion of the simulated image in which the sizes of the discs are log-normally distributed (A) and an enlargement (B).

variograms agree closely with one interesting difference. The observed variogram exhibits a more rounded shape than the explicit variogram for fixed disc size. This rounded shape can be understood by examining the effect of the distribution of sizes on the variogram. At small distances, the variogram is a little higher than expected, and at distances near the range of influence it is lower than expected. At short distances the existence of small discs causes an increased amount of perimeter for the same area covered, increasing the likelihood that movements of short distances will result in crossing a boundary. At distances near the range of influence, an opposite effect occurs. One result of the log-normal distribution is discs larger than the size of the fixed discs of the explicit variogram. These discs reduce the likelihood of crossing a boundary at distances smaller than their diameter, which can still be larger than the zone of influence of the fixed disc

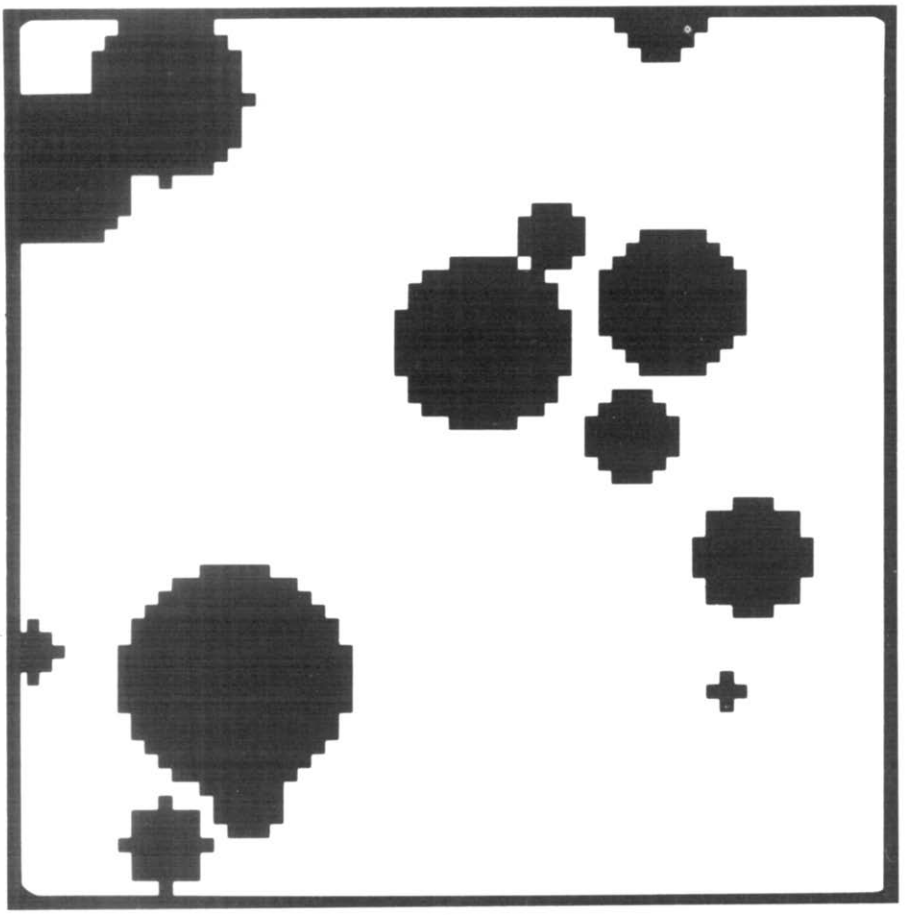

B

FIGURE 15. (Continued)

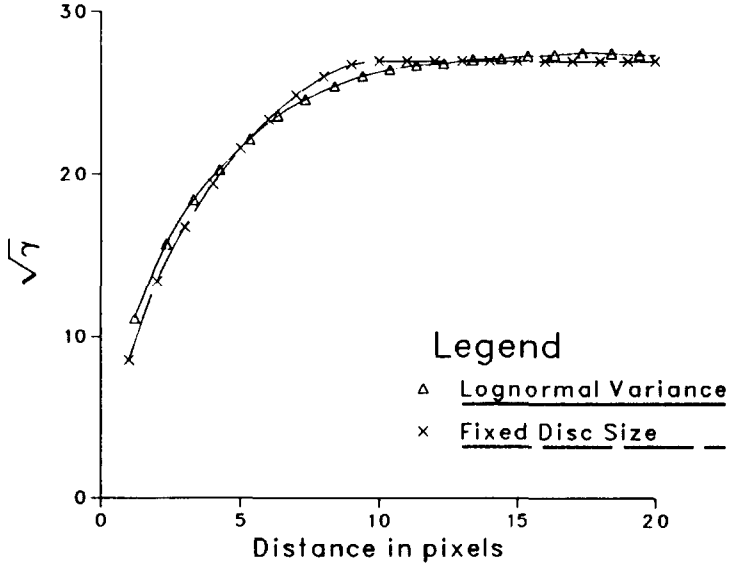


FIGURE 16. Comparison of the observed variogram from the simulated image with log-normal variance of disc sizes with an explicit variogram for a fixed size disc model.

model. This accounts for the difference between the two graphs in the 7–11-m range.

## 4. Discussion and conclusions

The main goal of the research presented in this paper was to establish a direct link between the spatial characteristics of images and the scene from which the image is derived. Variograms proved a useful tool for studying this link because they allow the problem to be approached from two different directions. By producing matching variograms by theoretical calculation of a regularized variogram and by empirical calculation of a variogram from a simulated image it was demonstrated that the spatial variation in images can be predicted on the basis of scene and sensor parameters. This "closing of the loop" between theoretical and empirical variograms for a specific scene model is probably the most significant finding of this research. This link between scenes, images, and spatial variation is essential for improving the use of spatial data in information extraction. It is only a preliminary step in a much larger process, but it is hoped that it will serve to alter people's perception of the nature of spatial variation in images. Through the use of scene models, spatial variation can be modeled for images. Empirical association is not the only way spatial variation in images can be studied.

In addition to "closing the loop," both ways of using variograms proved useful for understanding the nature and causes of spatial variation in images. The explicit variograms calculated for simple models of scenes showed that the characteristics of the variogram are related to the parameters of the scene model. For the disc model, the height of the sill is related to the number of discs (or density of coverage) and the distance to the sill is related to their diameter. Through the regularization process it is possible to calculate variograms as if they were derived from measurements of some length or area rather than from points. The effects on punctual variograms of regularization are to increase the zone of influence, decrease the height of the sill, and increase the height of the first measurement relative to the sill until they match. The effects of regularization are critical because they correspond to the effects imposed by the IFOV of a sensor capturing images of a scene. The regularization of punctual variograms allows the direct calculation of variograms as they would be measured in an observed image.

Empirical variograms of simulated images were used to test the effect of generalizing our simple disc model to consider the effect of the shape of objects in a scene and their size distribution. The effect of cone-shaped objects was minimal, while increasing the variance in their size distribution resulted in a more rounded shape near the range of influence of the variogram. The use of simulated images was particularly helpful for initial evaluation of observed variograms because scene parameters could be controlled and changes in variograms reliably related to those factors. The second paper in this series involves the empirical calculation of variograms from real digital images and attempts to apply the knowledge gained from this analysis to their interpretation.

*The authors would like to acknowledge the support of NASA under Grant NAS 9-16664, Subcontract L200080.*

## References


Bloomfield, P. (1976), *Fourier Analysis of Time Series: An Introduction*, Wiley, New York.

Box, G. E. P., and Jenkins, B. M. (1976), *Time Series Analysis, Forecasting, and Control*, Hoden-Day, San Francisco.

Clark, I. (1977) Regularisation of a semivariogram, Comput. Geosci. 3(2):341–346.

Clark, I. (1979), *Practical Geostatistics*, Applied Science, Essex, England.

Cliff, A. D., and Ord, J. K. (1981), *Spatial Processes: Models and Applications*, Pion, London.

Craig, R. G., and Labovitz, M. L. (1980), Sources of variation in Landsat autocorrelation, *Proc. of the 14th Int. Symp. on Remote Sensing of Environment*, San Jose, Costa Rica, pp. 1755–1767.

Davis, L. (1981), Polarograms: a new tool for image texture analysis, *Pattern Recognition* 13(3):219–223.

Frank, T. D. (1984), The effect of change in vegetation cover and erosion patterns on albedo and texture of Landsat images in a semiarid environment, *Ann. Assoc. Am. Geogr.* 74(3):393–407.

Franklin, J., Michaelson, J., and Strahler, A. H. (1985), Spatial analysis of density dependent patterns in coniferous forest stands, *Vegetatio* 64:26–36.

Glass, L., and Tobler, W. R. (1971), Uniform distribution of objects in a homogeneous field: cities on a plain, *Nature* 233:67–68.

Haining, R., Griffith, D. A., and Bennett, R. (1983), Simulating two-dimensional autocorrelated surfaces, *Geogr. Anal.* 15(3): 247–255.

Haralick, R. M. (1979), Statistical and structural approaches to image texture, *Proc. IEEE* 67(5):768–804.

Jupp, D. L. B., Strahler, A. H., and Woodcock, C. E. (1988), Theory of autocovariance and regularization in digital images, *IEEE Trans. Geosci. Remote Sens.*, forthcoming.

Kisiel, C. C. (1969), Time series analysis of hydrologic data, *Adv. Geosci.* 5:1–119.

Labovitz, M. L., Toll, D. L., and Kennard, R. E. (1981), Preliminary evidence for the influence of physiography and scale upon the autocorrelation function of remotely sensed data, NASA TM 82064, Goddard Space Flight Center, Greenbelt, MD.

Li, X. (1981), An invertible coniferous forest canopy reflectance model, Masters thesis, Department of Geography, University of California, Santa Barbara.

Li, X., and Strahler A. H. (1985), Geometric-optimal modeling of a conifer forest canopy, *IEEE Trans. Geosci. Remote Sens.* GE-23:705–721.

Matern, B. (1960), Spatial variation, *Medd. Statens Skogsforskningsinst.* 49:1–144.

Matheron, G. (1971), *The Theory of Regionalized Variables and Its Applications*, Les Cashiers du Centre de Morphologie Mathematique de Fontainebleau.

Mollering, H., and Rayner, J. N. (1981), The harmonic analysis of spatial shapes using dual axis fourier shape analysis (DAFSA), *Geogr. Anal.* 13(1):64–77.

Oden, N. L. (1984), Assessing the significance of a spatial correlogram, *Geogr. Anal.* 16(1):1–16.

Olson, J. M. (1975), Autocorrelation and visual map complexity, *Ann. Assoc. Am. Geogr.* 65:189–204.

Rayner, J. N. (1971), *An Introduction to Spectral Analysis*, Pion, London.

Serra, J. (1982), *Image Analysis and Mathematical Morphology*, Academic, New York.

Shih, E., and Schowengerdt, R. (1983), Classification of arid geomorphic surfaces using

Landsat spectral and textural features, *Photogramm. Eng. Remote Sens.* 3: 337–347.

Strahler, A. H., Woodcock, C. E., and Smith, J. A. (1986), On the nature of models in remote sensing, *Remote Sens. Environ.* 20:121–139.

Weszka, J. S., Dyer, C. R., and Rosenfeld, A. (1976), A comparative study of texture measures for terrain classification, *IEEE Trans. Syst. Man Cybern.* SMC-6(4):269–287.

*Received 9 November 1987; revised 16 April 1988.*